HIV-1 hypermethylated guanosine cap licenses specialized translation unaffected by mTOR

Gatikrushna Singh[a,1,2], Bradley Seufzer[a], Zhenwei Song[b], Dora Zucko[a], Xiao Heng[b,2], and Kathleen Boris-Lawrie[a,2]

[a]Department of Veterinary and Biomedical Sciences, University of Minnesota—Twin Cities, Saint Paul, MN 55108; and [b]Department of Biochemistry, University of Missouri, Columbia, MO 65211

Edited by Stephen Goff, Department of Chemistry and Molecular Biophysics and Department of Microbiology and Immunology, Columbia University Irving Medical Center, New York, NY; received March 18, 2021; accepted November 4, 2021

Appended to the 5′ end of nascent RNA polymerase II transcripts is 7-methyl guanosine (m^7G-cap) that engages nuclear cap-binding complex (CBC) to facilitate messenger RNA (mRNA) maturation. Mature mRNAs exchange CBC for eIF4E, the rate-limiting translation factor that is controlled through mTOR. Experiments in immune cells have now documented HIV-1 incompletely processed transcripts exhibited hypermethylated m^7G-cap and that the down-regulation of the trimethylguanosine synthetase-1–reduced HIV-1 infectivity and virion protein synthesis by several orders of magnitude. HIV-1 cap hypermethylation required nuclear RNA helicase A (RHA)/DHX9 interaction with the shape of the 5′ untranslated region (UTR) primer binding site (PBS) segment. Down-regulation of RHA or the anomalous shape of the PBS segment abrogated hypermethylated caps and derepressed eIF4E binding for virion protein translation during global down-regulation of host translation. mTOR inhibition was detrimental to HIV-1 proliferation and attenuated Tat, Rev, and Nef synthesis. This study identified mutually exclusive translation pathways and the calibration of virion structural/accessory protein synthesis with de novo synthesis of the viral regulatory proteins. The hypermethylation of select, viral mRNA resulted in CBC exchange to heterodimeric CBP80/NCBP3 that expanded the functional capacity of HIV-1 in immune cells.

RNA fate | virus–host interaction | m7G-cap methylation | eIF4E inactivation | nuclear RNA helicase

During transcription by RNA polymerase II, the 5′ end of nascent RNAs is covalently modified by monomethylated guanosine (m^7G-cap) (1), and the m^7G-cap binds the nuclear cap-binding complex (CBC) (2). Both capping and CBC acquisition are prerequisites for the assembly of ribonucleoproteins (RNPs) that catalyze RNA processing and facilitate nuclear export and cap-dependent translation (3). CBC is heterodimeric CBP80 tethered to the m^7G-cap by CBP20/NCBP2 (4). The m^7G-cap of select, RNA Pol II–transcribed RNAs can be hypermethylated at the N2 position of guanosine to create a trimethylguanosine 2, 2, 7-capped RNA (TMG-cap). The most well-defined substrates of TGS1 are small nuclear RNA, small nucleolar RNA, and telomerase RNA (5). Selected HIV-1 RNAs exhibit TMG-caps that has been identified to promote Rev/Rev-responsive element (RRE)–dependent posttranscriptional expression, although the role in viral replication has remained unanswered for a decade (6). More recently, TGS1 has been shown to hypermethylate selected selenoprotein messenger RNAs (mRNAs) (5) that are oxidative stress reducers, anti-inflammatory actors, and facilitators of wound healing (7). Translation of HIV-1 Rev/RRE-dependent mRNAs or selenoprotein mRNAs maintains during eIF4E down-regulation, but the translation mechanism remains controversial (8–10).

Cap exchange is the replacement of CBC with eIF4E, the rate-limiting translation initiation factor for global protein synthesis (11). eIF4E serves as a central node for translation of mRNA templates involved in proliferation and survival (12, 13). eIF4E requires activation of serine–threonine kinase mTOR (mechanistic target of rapamycin) to phosphorylate 4E-BP1. Hypophosphorylated 4E-BP1 is the allosteric repressor of eIF4E binding that promptly attenuates m^7G-capped mRNA-to-protein translation (13–16). mTOR-regulated translational control couples immune cell signaling to the inflammatory response and is fundamental to effective antiviral response (17).

Recent studies have challenged the dictum that cap-dependent translation is exclusively attributable to eIF4E. At least 20% of host mRNAs have been shown to utilize eIF4GI homologs that bypass eIF4E binding to initiate translation [e.g., DAP5 (18) and CTIF (19)]. Moreover, eIF3d binding the 5′ untranslated region (5′-UTR) of the c-jun early response mRNA has been shown to bypass eIF4E (20). The junD mRNA maintains translation during mTOR inhibition yet fails conventional tests for cap-independent translation by an internal ribosome entry mechanism (20). Recently, the heterodimeric CBP80/NCBP3 has been shown to assemble JUND polysomes (21). The CBP80-NCBP3 heterodimer had been characterized in conditions of metabolic stress and viral infection and has been assigned roles in antiviral defense and RNA export that remain under investigation (22, 23). An emerging paradigm

Significance

The proliferation of viral pathogens is restricted by hosts, but resilient pathogens antagonize the restriction by hosts. Findings explain that HIV-1 blocked mono-methylated guanosine cap by hypermethylation and engaged novel cap-binding complex for virion protein translation unaffected by global translation inhibition. The hypermethylated cap activity required RNA-structure-dependent binding of RNA helicase A/DHX9. eIF4E interaction proceeded on completely spliced HIV messenger RNA templates encoding viral regulatory proteins, thus eIF4E inactivation by catalytic site mTOR inhibitor suppressed regulatory protein translation, while structural/accessory protein translation was maintained. Two mutually exclusive translation pathways antagonize hosts and facilitate HIV-1 proliferation in primary $CD4^+$ T cells to the detriment of hosts. eIF4E inactivation imposed an operational rheostat that suppressed regulatory proteins, while maintaining virion production in immune cells.

Author contributions: G.S., K.B.-L., X.H., and Z.S. designed research; G.S., B.S., and Z.S. performed research; D.Z. contributed reagents and drawings; G.S., K.B.-L., B.S., X.H., and Z.S. analyzed data; and K.B.-L., G.S., X.H., and Z.S. wrote the paper.

The authors declare no competing interest.

This article is a PNAS Direct Submission.

[1]Present address: Department of Neurosurgery, University of Minnesota, Minneapolis, MN 55455.

[2]To whom correspondence may be addressed. Email: kbl@umn.edu, gsingh@umn.edu, or hengx@missouri.edu.

This article contains supporting information online at http://www.pnas.org/lookup/suppl/doi:10.1073/pnas.2105153118/-/DCSupplemental.

Published December 23, 2021.

posits alternative, cap-binding proteins, and select mRNA templates engage in specialized translation pathways that are unaffected by global down-regulation of translation, ultimately providing polypeptides important for stress responsiveness and recovery from down-regulation of eIF4E-dependent translation.

HIV-1 primary RNA is processed into three classes of mature viral transcripts (24). Early HIV-1 gene expression is characterized by alternative splicing of HIV-1 primary RNA to multiply spliced (MS) transcripts encoding Tat, Rev, or Nef. The newly synthesized Rev binds RRE within the unspliced (US) and singly spliced (SS) RNAs to transactivate CRM1-dependent nuclear export of incompletely spliced viral transcripts (25). TGS1 was shown to hypermethylate the 5′-caps of the Rev/RRE-dependent HIV-1 RNAs and enhance CRM-1–dependent posttranscriptional expression by a process that remains poorly understood (6). Other investigations identified that the Rev/RRE-dependent HIV-1 RNAs fail cap exchange to eIF4E and engage polysomes composed of CBP80 and DHX9/RNA helicase A (RHA) (10, 26). Herein, we evaluated the following question: What is the role of hypermethylated caps and host cap-binding proteins in HIV-1 translation control?

Results

Hypermethylation of HIV-1 m^7-G Cap Significantly Bolsters Infectious Virus Production. TGS1 down-regulation studies were conducted in HeLa cells transfected with TGS1 small interfering RNA (siRNA) or nontargeting siRNA (siNT) for 24 h followed by HIV^{NL4-3} transfection for 24 h. The cell lysates and cell-free culture medium were collected, and Western blot (WB) of cell lysates validated that TGS1 was down-regulated by the specific siRNA, whereas the Tubulin-loading control was maintained (Fig. 1*A*). Gag ELISA (enzyme-linked immunosorbent assay) identified that siRNA-targeting TGS1 (siTGS1) treatment reduced Gag in culture medium to 10% of the control (Fig. 1*A*, *Bottom*). RNA was isolated from the cells and subjected to RT-qPCR with HIV-1 and control primer pairs. The results from three independent experiments demonstrated that the copies of HIV-1 US mRNA and control host RNAs were similar between siNT- and siTGS1-treated cells, suggesting that TGS1 down-regulation had diminished Gag translation efficiency (Fig. 1*B*). Next, these RNA samples were incubated with the commercial, TMG-specific antibody (6), and immunoprecipitation (IP) was conducted. The IP eluates and flow-through (FT) RNAs were subjected to RT-qPCR. The HIV-1 US transcripts were enriched in TMG precipitates compared to FT (Fig. 1*B*, row 1). Taken relative to input, TMG IP enriched HIV-1 US (80%) and positive control Sno-U3 (95%) and SelR transcripts (75%) in siNT-treated cells (Fig. 1*B*, row 1). After the TGS1 down-regulation, these transcripts enriched in the FT and TMG IP collected less than 5% of input (Fig. 1*B*, row 2). The results recapitulated prior findings that HIV-1 US RNAs exhibit m^7G hypermethylation attributable to TGS1 (6).

Next, MT-4 T cells were spinoculated with virus samples normalized to Gag p24. After 6 h, cells were washed, and the cells were cultured for 48 h. Results from three independent experiments demonstrated that TGS1 down-regulation significantly reduced infectivity of normalized virus (factor of ≥1,000) (Fig. 1*C*). We concluded the hypermethylation of HIV-1 m^7-G cap significantly bolsters infectious virus production, and the drastic effect involves translation control.

HIV-1 TMG-Capped US/SS mRNAs Fail to Enrich eIF4E and Engage NCBP3. Since TGS1 adds methyl groups to the m^7G cap that may disrupt eIF4E interaction, the TMG-cap of Rev-RRE–dependent mRNAs may engage a different cap-binding protein. Indeed, the polysomes of HIV-1 Rev/RRE-dependent RNAs have failed to enrich eIF4E and instead engage a CBP80 mRNP (27). Recently, NCBP3/CBP80 heterodimer has been shown to assemble JUND polysomes for cap-dependent translation without eIF4E (21). To test whether TMG-capped HIV-1 mRNPs enriched eIF4E or NCBP3, the messenger ribonucleoproteins (mRNPs) were collected from HIV-infected, primary $CD4^+$ T lymphocytes and subjected to RT-qPCR, as summarized in Fig. 2*A*. The RT-qPCR readily detected the HIV-1 US, SS, MS, and GAPDH RNA

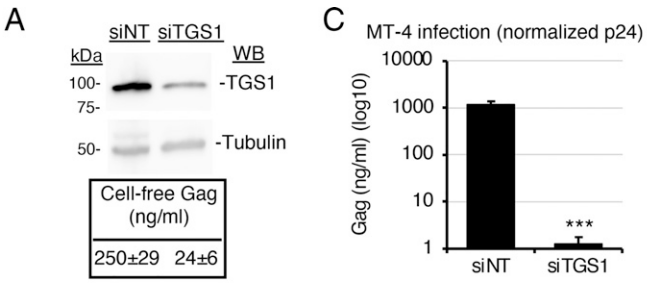

B

siRNA	RNA copies ×10⁴ (% of Input)											
	Input				Trimethylguanosine-IP				Flow Through			
	HIV US	Sno U3	Sel R	GAP DH	HIV US	Sno U3	SelR	GAP DH	HIV US	Sno U3	SelR	GAP DH
NT	290 ±58	253 ±29	40 ±4	253 ±32 (100)	227±25 (80)	241±34 (95)	30±5 (75)	<MD	7±0.3 (1)	9±2 (1)	<MD	216±18 (90)
TGS1	335 ±37	265 ±14	32 ±9	245 ±39	18±0.9 (5)	5.8±1 (1)	0.6±.03 (5)	<MD	217±31 (75)	264±28 (99)	27±8 (80)	241±37 (99)

Fig. 1. Hypermethylation of HIV-1 m^7-G cap significantly bolsters infectious virus production. HeLa cells were transfected with siTGS1 or siNT for 24 h and then HIV^{NL4-3}. Around 24 h later, cell lysates and cell-free culture media were collected for analyses. (*A*) Western blot of cell lysates with antiserum against TGS1 or the loading control tubulin and results of Gag ELISA on cell-free medium (box). Data are representative of three experiments. (*B*) RNA was isolated from the cells treated with siNT or siTGS1 followed by isolation of TMG immune complexes (IP) or IgG control. RT-qPCR using random hexamer and gene-specific primers detected HIV-1 US RNA, SnoU3, or SelR RNA in the input, TMG IP, and FT samples relative to IgG control. RNA copies were calculated relative to standard curves with detection limit of sensitivity 10^2 copies and the distribution in IP or FT was compared to Input; (), percentage of Input. (*C*) MT-4 cells were spinoculated with equivalent Gag (200 ng) from supernatant of HeLa cells experiencing TGS1 down-regulation (from *A*). After 48 h, MT-4 culture medium was collected and subjected to Gag ELISA. Gag production (log10) from three independent experiments with SD and significance determined by Student's *t* test (***$P < 0.001$).

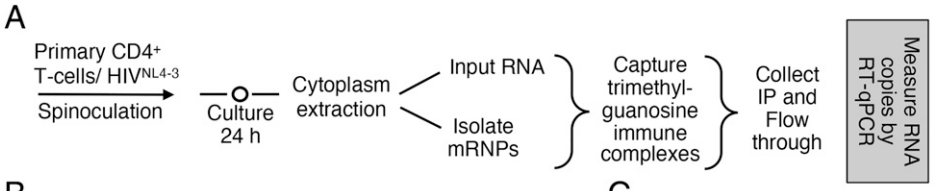

B

RNA copies ×10³	US	SS	MS	GAPDH
Input cytosol	207±25	138±27	203±34	370±29
NCBP3 RNP	270±31	180±29	<MD	<MD
eIF4E RNP	<MD	<MD	284±65	158±35

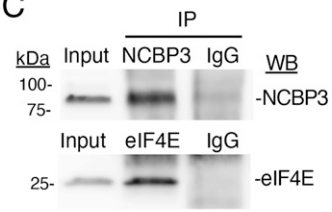

D

RNA copies ×10³ (% Input)	Trimethylguanosine-IP				Flow Through			
	US	SS	MS	GAPDH	US	SS	MS	GAPDH
Input cytosol	170±34 (82)	109±39 (79)	<MD	<MD	<MD	<MD	145±24 (71)	267±27 (72)
NCBP3 IP	167±29 (62)	154±31 (85)	<MD	<MD	<MD	<MD	<MD	<MD
eIF4E IP	<MD	<MD	<MD	<MD	<MD	<MD	174±61 (61)	128±55 (81)

Fig. 2. TMG-capped HIV-1 US/SS transcripts are components of NCBP3 mRNP and fail to enrich eIF4E. Primary CD4$^+$ T cells were infected with HIV^{NL4-3} (multiplicity of infection = 1), mRNPs were isolated, and coprecipitated RNAs were quantified by RT-qPCR with gene-specific primers. (*A*) Approach used to collect cytosolic NCBP3- and eIF4E mRNPs and hypermethylated RNAs by IP with antiserum specific to NCBP3, eIF4E, or TMG. Around 10% of input and entire IP samples were subject to RT-qPCR. (*B*) RNA copies in input samples, NCBP3, or eIF4E mRNPs were determined relative to standard curves and normalized to IgG-negative control. (*C*) Western blot of input lysate and isolated immune complexes by antiserum to NCBP3 or eIF4E. (*D*) Enrichment of TMG-capped RNAs from the Input or NCBP3 or eIF4E mRNP has been calculated. (), percentage (from *B*).

copies in the input cytoplasm (Fig. 2*B*, row 1). Immunoblotting validated the IPs enriched NCBP3 or eIF4E relative to IgG controls (Fig. 2*C*). HIV-1 US and SS transcripts were readily detectable in the NCBP3 IP, whereas MS or GAPDH RNAs were less than minimum detectable (<MD) (Fig. 2*B*, row 2). HIV-1 MS or GAPDH RNAs were readily detectable in the eIF4E RNP, whereas US or SS transcripts were <MD (Fig. 2*B*, row 3), indicating the HIV-1 Rev/RRE-dependent US/SS RNAs, and the MS RNAs were components of distinct mRNPs, as suggested previously (8).

Next, the RNA samples were incubated with a commercial, TMG-specific antibody (6), and the IP eluates and FT RNAs were subjected to RT-qPCR. The HIV-1 US/SS transcripts were enriched in TMG precipitates but not FT (Fig. 2*D*, row 1). Moreover, HIV-1 TMG-capped, Rev/RRE-dependent transcripts were components of the NCBP3 mRNPs (Fig. 2*D*, row 2). Input MS and GAPDH transcripts failed precipitation by TMG antiserum (Fig. 2*D*, row 1). As expected, MS and GAPDH transcripts were in the eIF4E mRNPs collected in the FT, verifying failed precipitation by TMG antiserum (Fig. 2*D*, row 3). The results confirmed and extended the prior observations that HIV-1 Rev/RRE-dependent US/SS RNAs are TMG-capped, whereas HIV-1 MS transcripts are not (6). We concluded that NCBP3 mRNPs engaged TMG-capped HIV-1 US/SS mRNA, whereas eIF4E mRNPs engaged MS transcripts and GAPDH. Given that the MS mRNAs, but not US/SS mRNAs, are components of eIF4E mRNPs, the results posited that mTOR regulates the translation of HIV-1 MS transcripts, whereas US/SS mRNAs are unaffected by mTOR. Hence, mTOR inhibition of HIV MS RNA translation would be expected to down-regulate Tat and Rev protein and diminish HIV proliferation.

mTOR Inhibition Down-regulates HIV-1 Regulatory Proteins. Torin-1 is a selective catalytic site mTOR inhibitor that up-regulates hypophosphorylated 4E-BP1 (21, 28, 29). Lymphocytes were infected with HIV^{NL4-3} for 6 h (multiplicity of infection [MOI] = 1), washed, and continuously cultured with or without Torin-1. The lowest dose of Torin-1 was selected (50 nM) that lacked off-target effects on cell viability while activating hypophosphorylated 4E-BP1 (21). At regular intervals, cell-free supernates were collected, and virus proliferation was measured by Gag ELISA. Torin-1 significantly diminished virus growth in primary CD4$^+$ T cells, and similar trends were observed in MT-4 and CEM×174 lymphocytes (*SI Appendix*, Fig. S1 *A–C*). The observed decline in HIV-1 proliferation by Torin-1 agreed with prior studies with mTOR inhibitors in HIV-infected cells attributed to defective Tat activity (30–33). To determine changes in proviral RNA levels, CEM×174 RNA was harvested from day 2 to the peak of virus proliferation, and RT-qPCR was performed. At day 2 and 4, HIV-1 US, SS, and MS RNA copies and control GAPDH RNA copies were similar in cultures with or without Torin-1 (*SI Appendix*, Fig. S1 *D–G*). By day 6, US RNA copies in Torin-1 cultures dropped by two orders of magnitude (*SI Appendix*, Fig. S1*D*), whereas the completely processed MS RNA displayed an upward trend (*SI Appendix*, Fig. S1*F*). The HIV-1 SS and GAPDH RNA copies remained similar irrespective of Torin-1, indicating no change in steady state (*SI Appendix*, Fig. S1 *E* and *G*). Prior research has shown that Rev/RRE transactivation does not affect the steady state of SS mRNAs but increases the steady state of US viral transcripts (34). We considered that the precipitous drop in US RNA in response to Torin-1 could be attributable to diminished regulatory protein synthesis.

CEM×174 cultures at day 4 postinfection were collected, and WB with anti–HIV-1 antibodies identified Torin-1–diminished, viral Tat, Rev, and Nef proteins and GAPDH, as observed in an earlier study (21) (*SI Appendix*, Fig. S1*H*). Env (gp160/gp120) and

Gag protein levels were unaffected by Torin-1, which could be attributable to longer protein half-lives or translation unaffected by Torin-1. To track the effect of Torin-1 on de novo protein synthesis, metabolic labeling of global protein synthesis for 30 min was performed with puromycin. WB of the cell lysates with puromycin verified that Torin-1 attenuated de novo protein synthesis (*SI Appendix*, Fig. S1*I*). The GAPDH antiserum documented that the attenuation of GAPDH synthesis was recapitulated (*SI Appendix*, Fig. S1 *H* and *I*). To measure the de novo synthesis of proteins from the HIV-1 US RNA, Gag antiserum was used for IP, and the immunoprecipitants were subjected to WB with puromycin antiserum. The results documented that de novo synthesis of puromycin-labeled Gag protein was similar in cultures with/without Torin-1 (*SI Appendix*, Fig. S1*I*). We concluded that mTOR inhibition attenuates HIV proliferation and down-regulates protein synthesis from the MS mRNAs, and the translation of HIV-1 US/SS mRNAs was unaffected by mTOR. Taken together, results posited that hypermethylated HIV-1 mRNAs undergo CBC exchange to CBP80/NCBP3 to assemble polysomes.

CBP80 and CBP20 (also known as NCBP1) form the heterodimeric CBC that binds nascent transcripts and is exchanged for eIF4E in the cytoplasm, whereas CBP80 and NCBP3 form an alternative CBC that has been identified to assemble JUND polysomes (21). To test whether HIV-1 hypermethylated RNAs assemble polysomes composed of CBP80 with CBP20 or NCBP3, siRNAs targeting CBP20, NCBP3, or nontargeting control, siNTs were transfected to human embryonic kidney 293 (HEK293) cells for 48 h, followed by HIV^{NL4-3} transfection for an additional 24 h. Cytoplasmic samples were collected, and WB-validated CBP20 and NCBP3 were down-regulated by the specific siRNAs relative to siNT (*SI Appendix*, Fig. S2*A*). Polysome profiling demonstrated that the individual down-regulation of CBP20 or NCBP3 increased the mass and number of polysomes, compared to mock treated, that may be attributable to increased ribosomal loading or reduced ribosome transit time on select mRNAs (*SI Appendix*, Fig. S2*B*). Combined down-regulation of CBP20 and NCBP3 reduced the magnitude of polysomes to be less than the mock treatment, indicating ribosomal loading to be deficient in these cells.

Next, the sucrose gradient fractions were pooled, and RNA was isolated and subjected to RT-qPCR. The accumulation of the HIV-1 hypermethylated US/SS mRNAs in polysomes maintains upon individual down-regulation of CBP20 or NCBP3, whereas dual down-regulation of CBP20 and NCBP3 retains the HIV-1 US/SS mRNA in preinitiation complex (PIC), indicating ribosomal-loading fails (*SI Appendix*, Fig. S2*C*). No change was identified in the distribution of MS or GAPDH RNAs, as expected by the observation that they assemble eIF4E mRNPs and do not assemble NCBP3 mRNPs (Fig. 2*B*).

To verify that the HIV-1 hypermethylated US/SS RNAs form CBP80/NCBP3 mRNPs for ribosomal loading, polysomes were collected, and CBP80 immunoprecipitants were subjected to WB. In polysomes from cells experiencing siNT, CBP80 coprecipitates NCBP3, but CBP20 is not detectable (*SI Appendix*, Fig. S2*D*). CBP20 siRNA down-regulates CBP80 coprecipitation of CBP20 and slightly increases NCBP3. The NCBP3 siRNA up-regulates CBP80-CBP20 heterodimers. In each case, the CBP80 mRNP contains RHA (Fig. 2*D*) and US/SS transcripts (*SI Appendix*, Fig. S2*E*). The dual down-regulation of NCBP3 and CBP20 abrogates detectable HIV-1 polysomal RNA. As expected, CBP80 mRNP fails to enrich MS or GAPDH transcripts. The results indicate that CBP20 and NCBP3 binding to CBP80 are likely mutually exclusive. None of the candidate proteins are detected in IgG control. We concluded that the HIV-1 hypermethylated RNAs assemble polysomes composed of CBP80/NCBP3-RHA mRNPs.

Rev/RRE-Dependent RNA Translation Is Attributable to CBP80/NCBP3-RHA mRNP. Recently, we identified that RHA is necessary to tether JUND–CBP80/NCBP3 mRNPs to polysomes. We also found that JUND translation is unaffected by Torin-1 unless RHA was down-regulated by siRNA (21). Prior research has shown that RHA down-regulation diminishes HIV-1 translation and virion infectivity (35–38). Thus, we sought to determine if RHA down-regulation diminishes hypermethylated HIV-1 RNAs. Cells were treated with siRNA-targeting RHA (siRHA) or nontargeting control (NT siRNA) for 24 h, followed by HIV^{NL4-3} transfection for 24 h. Cells were cultured with Torin-1 (50 nM, 18 h). Cytoplasm was collected, and WB was performed to validate the specific down-regulation of RHA compared to siNT control (Fig. 3*A*). Antiserum to 4EBP1 and phosphorylated 4EBP1 T37/46 validated that Torin-1 up-regulates total 4E-BP1 and down-regulates hyperphosphorylated α and β isoforms, indicating activation of the allosteric inhibitor of eIF4E. We observe that RHA down-regulation slightly diminishes total 4EBP1, and this observation remains to be investigated. With or without RHA down-regulation, we observed that Torin-1 reduces p-4EBP1 by a factor of 10 (Fig. 3*A*, right panel, bottom line). RHA, NCBP3, CBP80, and Tubulin did not turn over within the 18-h Torin-1 treatment, as expected from prior results (21). We noticed CBP80 increases in Torin-1 and siRHA treatment, and this remains to be investigated further. Lysate was reserved for polysome profiling and for isolation of RNA to be input for TMG-IP and RT-qPCR.

RT-qPCR performed on input RNA samples identifies that HIV-1 US, host SnoU3, SelR, or GAPDH copies were similar regardless if the cells experienced siRHA or siNT (Fig. 3*B*, *Top row*). In the TMG-IP, HIV-1 US and positive control SnoU3 and SelR readily detect in the siNT samples, and negative control GAPDH accumulates in FT samples (Fig. 3*B*, row 1). In the TMG-IP of siRHA samples, HIV US, SnoU3, or SelR RNA copies accumulate in FT, as do negative control GAPDH (Fig. 3*B*, row 2). We concluded that RHA down-regulation significantly diminishes the accumulation copies of hypermethylated transcripts yet does not diminish steady state.

The polysome profiling of siNT-treated cells showed that HIV-1 US/SS mRNA enrich in polysomes regardless of Torin-1 treatment (Fig. 3*C*, light green versus gold bars). RHA down-regulation fails to affect MS and GAPDH (blue bars), whereas US/SS mRNA accumulates in PIC in a pattern similar to MS mRNAs in Torin-1–treated cells (gold bars). We concluded that RHA down-regulation restricts accumulation of hypermethylated HIV-1 US/SS mRNAs suitable for specialized translation. The results suggested that RHA may be important for the acquisition of TGS1. Thus, we carried out reciprocal coprecipitation assays. Results with specific antiserum demonstrated that TGS1 readily coprecipitates RHA, and RHA coprecipitates TGS1 (Fig. 3*D*). In the TGS1 coprecipitate, RHA WB identifies a slightly smaller species of RHA that remains to be investigated. Recently, RHA has been shown to assemble JUND polysomes unaffected by mTOR (21); thus, experiments were warranted to characterize components of TMG-capped HIV-1 mRNPs in polysomes.

Translation of the Hypermethylated HIV-1 mRNAs Is Attributable to CBP80/NCBP3-RHA mRNPs. Polysomes were isolated on sucrose gradients and incubated with antiserum to CBP80 or eIF4E. Immune precipitates were washed, and equal aliquots were reserved for WB or RNA extraction and RT-qPCR. WB validated effective CBP80 and eIF4E IPs compared to the isotype-matched IgG control serum (*SI Appendix*, Fig. S3*A*, *Left*). CBP80 coprecipitates NCBP3 and RHA regardless of Torin-1 treatment, as had been observed previously (21). The CBP80 polysomes fail to coprecipitate detectable CBP20, eIF4E, or eIF4G. eIF4E coprecipitates eIF4G without Torin-1, and the proteins become undetectable with Torin-1.

Coprecipitating RNAs were extracted from CBP80 and eIF4E RNPs and subjected to RT-qPCR with gene-specific primers.

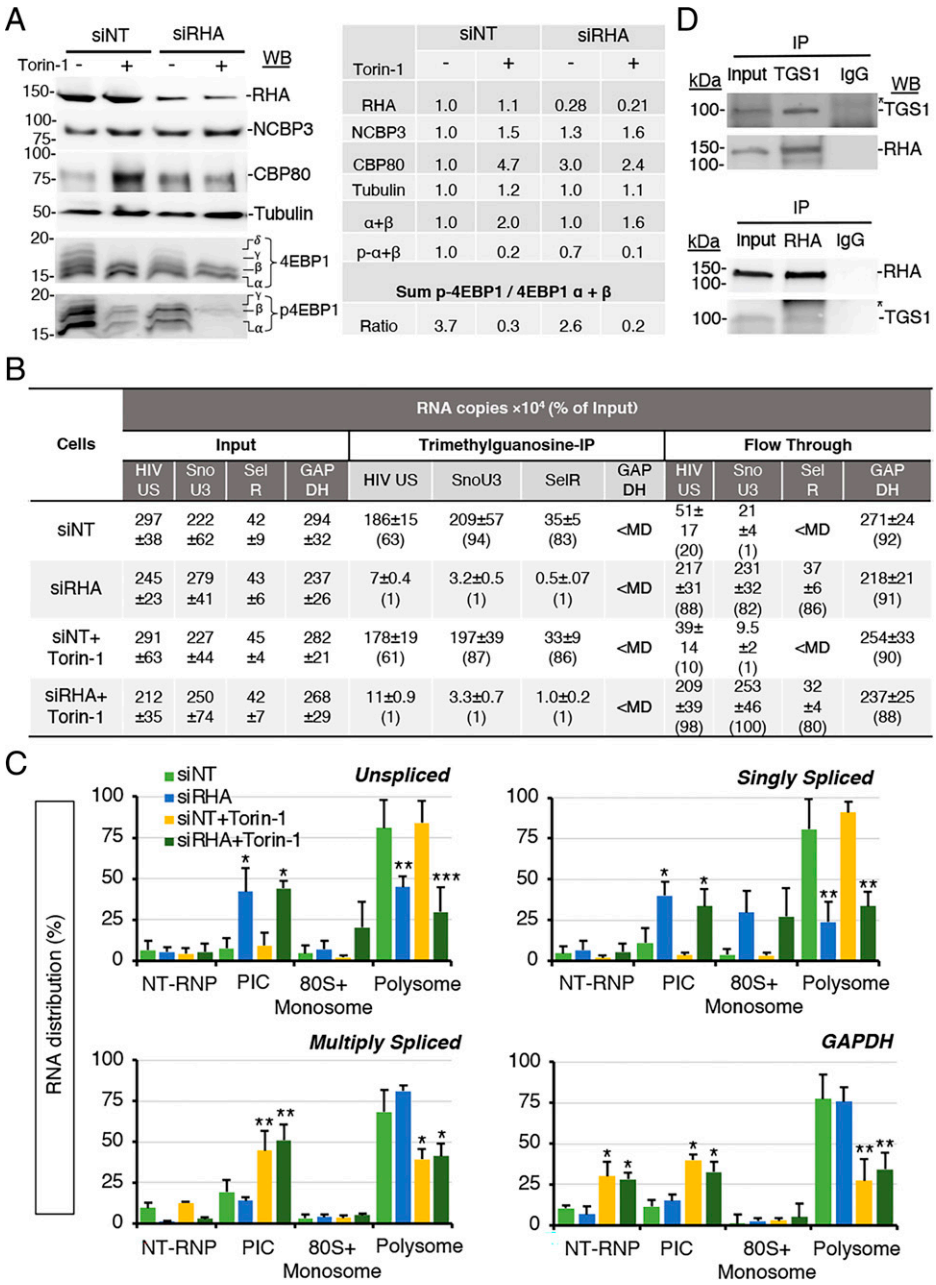

Fig. 3. RHA down-regulation restricts accumulation of hypermethylated HIV-1 US/SS mRNAs suitable for specialized translation. Analysis of HIV-1 mRNPs after siRNA down-regulation of RHA (siRHA) or nontargeting control (siNT). HEK293 cells experiencing siRNA for 24 h were transfected with HIV^{NL4-3} molecular clone for 24 h and then incubated with Torin-1 (50 nM) or control (0.2% DMSO) for 24 h. Cell lysates were subjected to WB or ribosomal profile analysis, and input RNA was extracted and incubated with antiserum to TMG. (*A*) WB was carried out with the indicated antiserum, and signals were quantitated (*SI Appendix*, Table S7) and summarized in the table panel. (*B*) TMG-capped RNAs were isolated from input. Precipitants and FT were collected, and RT-qPCR measured RNA copies. RNA copies were determined relative to standard curves and normalized to IgG-negative control. (): Percent of Input. (*C*) Distribution of RNA copies in nontranslating (NT) RNP, PIC, and 80S+ monosome and polysomes. RNA copies were calculated relative to standard curves. Results represent the mean of three independent experiments (bar) with SD. Statistical significance is the following: $*P \leq 0.05$, $**P \leq 0.005$, and $***P \leq 0.001$. (*D*) Reciprocal coprecipitation assay performed using lysate from HIV-1–infected primary T cells, and antiserum to TGS1 and RHA. WB with indicated antiserum.

Results from six independent experiments identified that US/SS RNAs enrich the polysomal CBP80 RNPs, whereas MS and GAPDH transcripts were less than <MD (*SI Appendix*, Fig. S3*A*, *Right*). The polysomal eIF4E mRNPs enrich MS and GAPDH, and US and SS transcripts were <MD. Torin-1 does not interfere with US or SS polysomes, consistent with activity of an internal ribosome entry site (IRES) in prior studies (9, 33, 39–43), but down-regulates the eIF4E-dependent MS and GAPDH polysomes.

Antiserum to RHA was incubated with the polysome preparations, and coprecipitates enrich CBP80/NCBP3 and HIV-1 US/SS transcripts regardless of Torin-1 treatment. RHA-CBP80/NCBP3 mRNPs fail to enrich eIF4E, MS transcripts, or GAPDH transcripts (*SI Appendix*, Fig. S3*B*). The IgG control serum failed to detect RHA or HIV-1 transcripts validating specificity of the RHA coprecipitates (*SI Appendix*, Fig. S3*B*). We concluded that the hypermethylated US/SS mRNA assemble polysomes composed of CBP80/NCBP3-RHA mRNPs.

HIV-1 Specialized Translation Requires RHA Interaction with 5′-UTR at Primer Binding Site Segment. RHA interaction with the HIV-1 5′-UTR has been shown to promote HIV replication (37, 44, 45). Deletion of Tat transactivation response element (TAR) or the primer binding site (PBS) segment has been shown to eliminate RHA's interaction and activity as an HIV-1 dependency factor, indicating important roles for both RNA regions (37, 46). Recently, the PBS segment of the HIV-1 5′-UTR was demonstrated to form a three-way junction structure that conveys shape-specific recognition of RHA's double-stranded, RNA-binding domain I (46). Mutation A140C was sufficient to eliminate the three-way junction structure, and small-angle X-ray scattering (SAXS) data analysis identified an anomalous RNA structure (46). To verify the SAXS results, we employed NMR studies to compare the conformation of the PBS segment between WT and A140C and observed that the imino proton patterns of the A140C are different from that of the wild type (WT) (*SI Appendix*, Fig. S4), in agreement with the SAXS analysis showing that the point mutation causes drastic, secondary structural change (46). Next, we assessed RHA-binding affinity using recombinant full-length RHA (*SI Appendix*, Fig. S5*A*) titrated into WT PBS segment and A140C (*SI Appendix*, Fig. S5*B*) at various ratios by electrophoresis mobility shift assay (EMSA) (*SI Appendix*, Fig. S5*C*). We benchmarked the affinity of RHA binding to TAR-PolyA (nucleotide: nt-1 to 104), an RNA element of similar size as PBS segment that has been shown insufficient for RHA activity on the HIV-1 5′-UTR but likely affects the folding of downstream PBS segment in cellulo (44, 45).

Results of the EMSA demonstrated the affinity of recombinant RHA to PBS segment was greater than either A140C or TAR-PolyA. The EMSA data were fitted into the Hill–Langmuir equation, and the calculated microscopic dissociation constant K_d for PBS segment is 2.5 ± 0.04 μM, whereas A140C and TAR-PolyA reduce RHA affinity to similar K_d values (K_d = 5.5 ± 0.8 μM and 5.3 ± 0.2 μM, respectively) (*SI Appendix*, Fig. S5*D*). These results suggested that the anomalous structure of A140C supports nonspecific interaction that is insufficient for RHA activity in supporting HIV-1 replication in cellulo and agree with the previous identification of two RNA-binding modes of RHA (46): 1) selective PBS segment shape-specific RNA interaction as an HIV-1 dependency factor and 2) nonspecific interaction typified by TAR-PolyA and A140C that is attributable to electrostatic interaction of double-stranded RNA, with basic residues plentiful in the helicase core and arginine-rich C terminus of RHA for the general helicase function of RHA. The A140C molecular clone was introduced to cells, and we evaluated the possible down-regulation of HIV-1 hypermethylated US/SS mRNAs and restriction of specialized HIV-1 translation unaffected by mTOR.

We compared the activity of WT HIV^{NL4-3} with molecular clones A140C and ΔPBS, in which the PBS segment was deleted and replaced with a tetraloop (37) (Fig. 4*A*). The molecular clones were transfected to HEK293 cells for 6 h, and the cells were washed and cultured in medium with and without Torin-1. After 24 h, cell culture medium was supplemented with 200 pmol biotin–puromycin for 30-min metabolic labeling of global protein synthesis. WB with streptavidin–horseradish peroxidase (HRP) documented that Torin-1 down-regulated global protein synthesis (Fig. 4*B*, *Upper*), consistent with *SI Appendix*, Fig. S1*I*. Biotinylated proteins were captured using streptavidin and subjected to Gag WB. Biotinylated Gag-Pol and Gag proteins were readily detected from WT HIV^{NL4-3} irrespective of Torin-1 (Fig. 4*B*, *Middle*, lanes 2 and 3). In contrast, biotinylated Gag-Pol and Gag proteins from ΔPBS and A140C were down-regulated by Torin-1, just as observed for GAPDH. Densitometry of the WB signals (*SI Appendix*, Table S1) documented that mTOR inhibition also down-regulated ΔPBS and A140C translation. RNA was isolated from these cells, and RT-qPCR showed no change in steady-state HIV-1 or GAPDH RNA by Torin-1 (*SI Appendix*, Table S2). We concluded that the PBS segment of the 5′-UTR was important for specialized translation of the Rev/RRE-dependent, proviral RNAs. We postulated that A140C was sufficient to restrict HIV-1 cap hypermethylation and the assembly of CBP80-NCBP3-RHA into HIV-1 mRNPs.

HEK293 cells were transfected with WT HIV^{NL4-3} or A140C for 24 h, and RNA was collected and subjected to TMG-IP. RT-qPCR showed copies of WT and A140C RNA to be similar in the input samples (Fig. 4*C*). The TMG IP–positive control RNAs SnoU3 (77%) and SelR (60%) verified the integrity of the assay and that A140C US RNA copies accumulates in FT (94%), which indicates the dearth of TMG-cap. Taken together, with the observation that Torin-1 down-regulated A140C Gag translation, A140C was not expected to assemble CBP80/NCBP3-RHA mRNPs.

NCBP3/CBP80 RNPs and eIF4E-RNPs were examined for A140C RNA copies by RT-qPCR. The results verified that A140C US/SS RNAs fail the assembly of NCBP3 IPs (*SI Appendix*, Table S3*A*). A140C US/SS and MS transcripts and GAPDH devoid of TMG-caps readily detect in eIF4E mRNPs (*SI Appendix*, Table S3*B*). Since A140C derepressed cap exchange to eIF4E, Torin-1 treatment was expected to down-regulate A140C polysomes. Polysome analysis documented that A140C US/SS transcripts retain PIC similarly to the MS and GAPDH control transcripts in response to Torin-1 (*SI Appendix*, Fig. S6, compare minus and plus Torin-1). The results indicated A140C 5′-UTR fail assembly of CBP80/NCBP3 mRNPs in a manner similar to down-regulation of RHA or TGS1. We concluded that the dearth of hypermethylated m^7G-caps allows A140C cap exchange to eIF4E and

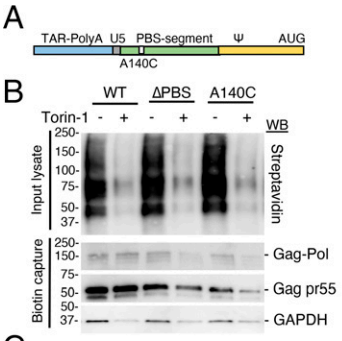

C

RNA IP	RNA copies (1×10⁴)											
	Input				Trimethylguanosine-IP				Flow Through			
	HIV US	Sno U3	Sel R	GAP DH	HIV US	Sno U3	Sel R	GAP DH	HIV US	Sno U3	Sel R	GAP DH
WT	277 ±61	267 ±57	78 ±13	261 ±29	214 ±55 (77)	205 ±64 (77)	63 ±15 (81)	<MD	15 ±2 (1)	8 ±1 (1)	<MD	227 ±48 (87)
A140C	271 ±79	272 ±84	94 ±39	265 ±33	0.06 ±0.01 (1)	209 ±51 (78)	56 ±24 (60)	<MD	255 ±81 (94)	12 ±3 (1)	27 ±7 (3)	223 ±57 (84)

Fig. 4. HIV-1 A140C structural perturbation of PBS-segment diminishes nuclear helicase binding and eliminates US/SS mRNA specialized translation unaffected by mTOR. (*A*) Diagram illustrating functional segments of HIV-1 5′-UTR. Colored bars: TAR, TAR-PolyA: blue (nt 1 to 104); unique 5′ (U5) (nt 105 to 124): gray; PBS segment: green (nt 125 to 225); core encapsidation signal, Ψ, and start codon (AUG) stem: tan (nt 226 to 356); and A140C: white box. (*B*) HEK293 cells were transfected with HIV^{NL4-3} or ΔPBS or A140C molecular clones for 24 h, cultured without (–) or with Torin-1 (50 nM) (+) for 18 h. For 30 min, cultures were supplemented with biotinylated puromycin. Cell lysates were collected, and equal volumes incubated with streptavidin, washed, collected, and subjected to WB with streptavidin–horseradish peroxidase (HRP), Gag, and GAPDH. (*C*) RNA isolated from transfected cells (in *B*) followed by TMG immune complexes (IP) isolation. RT-qPCR of HIV-1 US or cellular SnoU3 or SelR RNA in Input, TMG IP or FT samples. RNA copies were calculated relative to standard curves (range 10^2 to 10^8). (): Percent of Input.

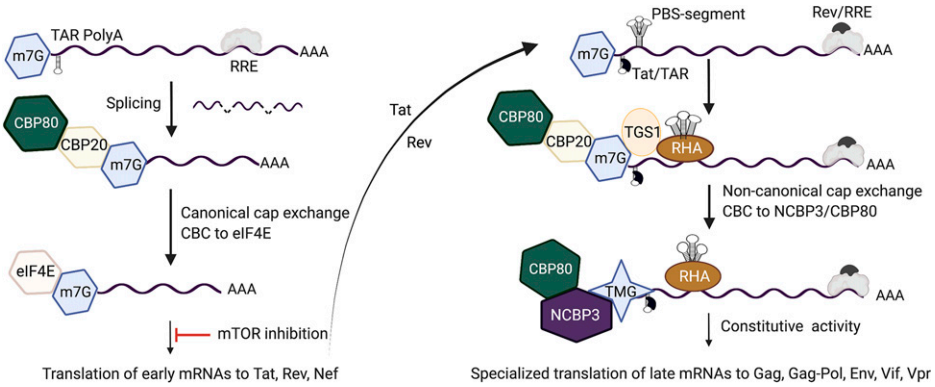

Fig. 5. HIV-1 MS mRNAs and US/SS mRNAs engage different translation pathways attributable to specific binding of nuclear RNA helicase (RHA) and m^7G-cap hypermethylation that inhibits CBC exchange to eIF4E and favors exchange to CBP80/NCBP3 mRNPs for specialized translation unaffected by mTOR. (*Left*) eIF4E-dependent translation of Tat, Rev, and Nef from fully processed HIV-1 mRNAs is controlled through mTOR. Nascent HIV-1 transcripts receive the monomethylated guanosine (m^7G) cap and 3′ polyadenylate tail (AAA) and are alternatively spliced. m^7G-cap is cotranscriptionally bound by CBC composed of CBP20-CBP80 and supports cap exchange to eIF4E. The mTOR substrate 4EBP1 is the allosteric inhibitor of eIF4E. (*Left*) mTOR hyperphosphorylates 4E-BP1 to activate global eIF4E-dependent mRNAs translation. mTOR inhibition (e.g., Torin-1) engenders hypophosphorylated 4E-BP1 and global repression of translation inclusive of Tat, Rev, and Nef. (*Right*) CBP80/NCBP3-RHA–specialized translation of HIV-1 structural and accessory proteins. HIV-1 late gene expression is characterized by Tat and Rev transactivation of nascent HIV-1 RNAs at the TAR and RRE, respectively. HIV-1 m^7G-cap is cotranscriptionally bound by CBC followed by folding of the 5′-UTR PBS segment three-way junction structure recognized by RHA. RHA engenders TGS1 hypermethylation of the m^7G-cap–inhibiting cap exchange to eIF4E. NCBP3/CBP80-RHA mRNP engage a specialized translation pathway for structural and accessory protein synthesis during down-regulation of global translation.

translation regulated by mTOR. We concluded that RHA–PBS segment shape-specific interaction was important for HIV-1 TMG-cap and specialized translation unaffected by mTOR.

Discussion

This study has demonstrated that two different translation mRNPs engage HIV-1 MS mRNAs and US/SS mRNAs and promote significant HIV-1 proliferation in primary $CD4^+$ T cells. HIV-1 MS transcripts undergo CBC exchange and eIF4E-dependent translation to regulatory proteins (Fig. 5, *Left*). The m^7G-cap of HIV-1 Rev/RRE-dependent transcripts experience hypermethylation that appears to be inhibitory to eIF4E exchange (Fig. 5, *Right*). The recruitment of TGS-1 for 5′-cap hypermethylation requires RNA helicase recognizing the shape of the 5′-UTR of the US/SS mRNAs. Selective RHA binding to the PBS segment promotes assembly of heterodimeric CBP80/NCBP3 mRNP that initiate viral structural/enzymatic and accessory protein synthesis unaffected by mTOR (Fig. 5, *Right*). The down-regulation of TGS1 or components of the CBP80/NCBP3/RHA mRNP or structural mutation of the PBS segment derepress eIF4E exchange. Our results show that the mutually exclusive translation mechanisms for HIV-1 MS mRNAs and US/SS mRNAs significantly bolster virion proliferation in immune cells.

Shutdown of the global eIF4E-dependent translation is integral to cell cycle progression and host restriction of infection. We recently reported a specialized translation of JUND mRNA that requires heterodimeric CBP80/NCBP3 for protein translation during global shutdown of eIF4E-dependent translation (21). NCBP3 has been assigned roles in antiviral defense and RNA export that remain under investigation (22, 23). Future experiments are warranted to understand the contribution of the CBP80/NCBP3/RHA translation pathway to the appropriate synthesis of innate response proteins and balanced proinflammatory responses.

Vpr is an HIV-1 accessory protein that significantly enhances HIV-1 proliferation in culture and in vivo by increased viral gene expression (19, 47). We have shown that Vpr mimics an mTOR inhibitor and inactivates eIF4E by promoting cell cycle arrest (10). We now propose that HIV-1 Vpr-induced inactivation of eIF4E prevents constitutive Rev synthesis that is important for balance between the accumulation of MS mRNAs encoding regulatory proteins and US/SS mRNAs encoding structural/enzymatic and accessory proteins in HIV-infected cells (Fig. 5).

Explanations for HIV-1 5′-UTR–driven translation of US/SS mRNAs have been mired in controversy for decades (48). Abundant literature has identified that in cellulo translation of HIV-1 late proteins continues during inactivation of eIF4E-dependent translation by host cell cycle arrest, nutrient deprivation (10, 39, 41), poliovirus (39), encephalomyocarditis virus (35), protease activity (49–51), or mTOR inhibitors (33, 40). HIV-1 translation during eIF4E inactivation was consistent with cap-independent translation by internal ribosome entry (42, 43, 48). We present unequivocal evidence that the translation of HIV-1 US/SS mRNAs is cap-dependent relying on TGS1, albeit by an alternative CBP80 heterodimer composed of CBP80/NCBP3. The down-regulation of CBP80/NCBP3-RHA mRNP derepressed CBC exchange to eIF4E and detained US/SS mRNAs in 48S complexes typical of defective ribosomal scanning.

CBC exchange to eIF4E was also derepressed by structural mutation of the PBS segment required for RHA activity on the 5′-UTR. The PBS segment three-way junction structure overlaps the previously identified stem loop, whose structural mutation inhibits HIV-1 IRES activity (IRES negative element) (11). Additional experiments will be required to reconcile whether acquisition of CBP80/NCBP3-RHA mRNP influences ribosome scanning, shunting, or internal ribosome entry to promote polysome loading.

The RNA tertiary structure near the 5′-cap is emerging as a major variable determining the fate of particular host and viral RNAs. The structure of the c-jun 5′-UTR inhibits cap exchange to eIF4E (20, 52) through sequestration of cap by eIF3d (20, 53, 54). HIV-1 nt–nt pairings within the PolyA region have been shown to modulate exposure of the HIV-1 m^7G-cap for eIF4E interaction (55, 56) and up-regulate HIV-1 translation rate in cells (57). Herein, nt–nt pairings within the PBS segment were shown to modulate activity of RHA, m^7G-cap hypermethylation, and retention of CBP80 for noneIF4E-dependent translation. HIV-1 PolyA and PBS segment overlap

the structure of the RHA-responsive posttranscriptional control element (PCE) identified in several retroviruses (35, 58, 59). Our data suggest that RHA/PCE influence the RNA folding in proximity to the 5′-cap determining the fate of particular host and viral RNAs.

All of the HIV-1 mRNAs (US/SS and MS) share the same 288 nucleotides at the 5′ terminus from +1 until the first splice donor site. They all contain the PBS segment as a potential RHA binding site for assembly of CBP80/NCBP3/RHA mRNPs. Our data suggested that the HIV-1 US/SS mRNAs engaged in CBP80/NCBP3-RHA translation RNPs expose PBS segment three-way junction structure for RHA recognition. However, disruption of the three-way junction redirected US/SS mRNAs to eIF4E RNPs devoid of RHA, similar to the MS mRNAs. Our results suggest that the 5′-UTR structures control epigenetic modification of the m^7G-cap and sort them into the separate translation pathways to ensure productive synthesis of HIV-1 structural/enzymatic/accessory proteins when hosts shutdown global translation in response to mTOR inhibition. Our results support the hypothesis that PBS segment regions are metastable determinants important for sorting MS mRNAs for eIF4E-dependent translation of regulatory proteins and US/SS transcripts for CBP80/NCBP3-RHA–dependent translation of virion proteins (56, 57, 60, 61).

Materials and Methods

Cells, Infections, siRNA, and Immunoblot. HIV^{NL4-3}-infected human primary $CD4^+$ or CEM×174 or MT-4 cells (5×10^5 cells in 1 mL Roswell Park Memorial Institute [RPMI]-1640) were seeded into 12-well plates and maintained with or without Torin-1 (50 mM) for 21 d. Fractions of culture supernatant (10%) were collected and replenished by fresh culture medium with or without Torin-1. Gag released to the culture medium was measured by Gag p24 ELISA (XpressBio). HEK293 cells were transfected to propagate molecular clones and for siRNA down-regulation (1×10^6 HEK293 cells per 35-mm well). SiRNA (50 nM) -targeting RHA (21), NCBP2, NCBP3, TGS1 (21, 22), or siNT were transfected with Lipofectamine 2000 (1 μL/10 nM siRNA) (Invitrogen) and Opti-minimum essential media (MEM) (500 μl); the medium was exchanged after 6 h and 24 h later. Cultures were supplemented with 0.2% DMSO or Torin-1 (50 nM) for 18 h followed by 2-mM puromycin treatment. Cytoplasmic protein or RNA was isolated in cell lysis buffer and TRIzol-LS (Ambion), respectively (21). Equivalent (20 μg) protein was subjected to WB with specific antibodies (*SI Appendix*, Table S1), and protein–antibody complexes were detected by enhanced chemiluminescence (GE Biosciences). Antibodies used in this study are listed in *SI Appendix*, Tables S4 and S5. Densitometry results were generated with ImageJ software (NIH).

Density Sedimentation, RNA IP, and RNA Analysis by qRT-PCR. Published protocols were used to perform density sedimentation and A_{254} spectrometry (21). For IP, Dynabeads Protein G (30 μL) (Invitrogen) were washed two times in 10-bed volumes of cytoplasmic lysis buffer (20 mM Tris·HCl [pH 7.4], 150 mM NaCl, 2 mM EDTA, and 1% Nonidet P-40) and antibodies (*SI Appendix*, Table S2) in 10-bed volume of IP lysis buffer (20 mM Tris·HCl [pH 7.4], 3 mM $MgCl_2$, 150 mM NaCl, 2 mM DTT, 1× protease inhibitor mixture EDTA free, 5 μL/mL RNase Out, 0.2 M sucrose, 0.5% Nonidet P-40, and 0.1% Triton X-100) with 1 mM bovine serum albumin (BSA) were incubated 45 min at room temperature. Bead–antibody complexes were washed in IP wash buffer (20 mM Tris·HCl [pH 7.4], 300 mM NaCl, and 0.5% Nonidet P-40) and incubated with 300 μg cell lysate at 4 °C for 2 h with rotation. Immune complexes were washed in IP wash buffer four times, and precipitates were collected by boiling with 1× SDS sample buffer or isolated in TRIzol-LS. Total RNA, cytoplasmic RNA, coprecipitated RNA by anti-NCBP1, eIF4E, or RHA was resuspended in ice-cold TMG IP buffer (20 mM Tris·HCl [pH 7.4], 150 mM NaCl, 0.1% Nonidet P-40, and 5 μL/mL RNase Out). TMG–antibody–bead complexes were washed and incubated with 5 μg RNA or all RNA-IP at 4 °C for 4 h with rotation, washed, and isolated in TRIzol-LS. As described previously, complementary DNA (cDNA) was generated using Omniscript (Qiagen), random primers (Invitrogen), and cellular or cytoplasmic RNA (2 μg) or coprecipitated RNA samples (62) followed by RT-qPCR using gene-specific primers (*SI Appendix*, Table S3).

RNA Purification, Recombinant Protein Purification, NMR Spectroscopy, and EMSA. $HIV\text{-}1^{NL4\text{-}3}$ PBS segment (nt 125 to 223 with two nonnative G–C pairs), PBS-A140C, and TAR-PolyA (nt 1 to 104) RNAs were synthesized by in vitro T7 transcription and purified by sequencing gel electrophoresis, elutrap elution, and salt washes (37). Recombinant RHA containing a Mocr-tag and His-tag at the N terminus was expressed in insect cells and purified as previously described (38). All NMR experiments were carried out using RNA concentrations ranging from 200 to 300 μM and preincubated in NMR buffer (10 mM Tris-d_{11} [pH 6.5] and 1 mM $MgCl_2$) at 37 °C for 1 h. One-dimensional proton spectra were collected for PBS segment and PBS-A140C in 90% H_2O and 10% D_2O at 283 K. All NMR data were collected on a Bruker Avance III 800MHz spectrometer equipped with TCI cryoprobe. For EMSA, the PBS segment, PBS-A140C, and TAR-PolyA RNA samples were refolded by preparing the RNA in 20 mM Hepes, pH 7.5, denaturing at 95 °C for 3 min, snap cooling on ice, and mixing with buffer to reach final concentration of 20 mM Hepes, pH 7.5, 140 mM KCl, and 1 mM $MgCl_2$ with 10% glycerol (buffer A). The RNAs were incubated at 37 °C for 30 min. The prefolded RNA was then mixed with recombinant RHA in buffer A to reach a final RNA concentration of 0.4 μM and protein concentrations of 0, 0.8, 1.6, 2.0, 2.4, 2.8, 3.2, 3.6, 4.0, and 4.8 μM, respectively. The mixtures were incubated at room temperature for 30 min and resolved on a 1.5% agarose gel ran at a constant voltage of 150 Volts for 45 min on ice. The EMSA experiment was repeated three times, and the representative EMSA gels are shown. The intensities of the bands in each gel were quantified in Image Laboratory (V6.1.0 build7, Bio-Rad Laboratories, Inc.). The binding affinity was calculated by fitting the data into the Hill–Langmuir equation (Origin 7.0).

Statistical Data Analysis. Three or more independent experiments were performed for each assay and results were combined to define the mean ± SD (SD). Statistical significance for comparisons between two sets of the experiments was assessed using unpaired two-tailed Student's *t* test, and a *P* value (*) of <0.05 was considered to be significant. For multiple treatment experiments, one-way ANOVA followed by multiple comparison analysis used GraphPad PRISM 8. Data were compiled in Microsoft Excel (2011). Statistical significance is the following: $*P \leq 0.05$, $**P \leq 0.005$, and $***P \leq 0.001$.

Data Availability. All study data are included in the article and/or *SI Appendix*.

ACKNOWLEDGMENTS. We thank Alon Herschhorn for the antiserum and NIH for Grant R01AI150460 to X.H. and K.B.-L.

1. Y. Furuichi, Discovery of m7G-cap in eukaryotic mRNAs. *Proc. Jpn. Acad. Ser. B. Phys. Biol. Sci.* **91**, 394–409 (2015).
2. T. Gonatopoulos-Pournatzis, V. H. Cowling, Cap-binding complex (CBC). *Biochem. J.* **457**, 231–242 (2014).
3. V. H. Cowling, Regulation of mRNA cap methylation. *Biochem. J.* **425**, 295–302 (2009).
4. E. Izaurralde *et al.*, A cap-binding protein complex mediating U snRNA export. *Nature* **376**, 709–712 (1995).
5. L. Wurth *et al.*, Hypermethylated-capped selenoprotein mRNAs in mammals. *Nucleic Acids Res.* **42**, 8663–8677 (2014).
6. V. S. R. K. Yedavalli, K.-T. Jeang, Trimethylguanosine capping selectively promotes expression of Rev-dependent HIV-1 RNAs. *Proc. Natl. Acad. Sci. U.S.A.* **107**, 14787–14792 (2010).
7. E. N. Reinke, D. N. Ekoue, S. Bera, N. Mahmud, A. M. Diamond, Translational regulation of GPx-1 and GPx-4 by the mTOR pathway. *PLoS One* **9**, e93472 (2014).
8. F. Carvajal *et al.*, Structural domains within the HIV-1 mRNA and the ribosomal protein S25 influence cap-independent translation initiation. *FEBS J.* **283**, 2508–2527 (2016).
9. K. Gendron, G. Ferbeyre, N. Heveker, L. Brakier-Gingras, The activity of the HIV-1 IRES is stimulated by oxidative stress and controlled by a negative regulatory element. *Nucleic Acids Res.* **39**, 902–912 (2011).
10. A. Sharma, A. Yilmaz, K. Marsh, A. Cochrane, K. Boris-Lawrie, Thriving under stress: Selective translation of HIV-1 structural protein mRNA during Vpr-mediated impairment of eIF4E translation activity. *PLoS Pathog.* **8**, e1002612 (2012).
11. A. Galloway, V. H. Cowling, mRNA cap regulation in mammalian cell function and fate. *Biochim. Biophys. Acta. Gene Regul. Mech.* **1862**, 270–279 (2019).
12. S. Fritz, K. Boris-Lawrie, The RNPs of eukaryotic translation control. *Trends Cell Mol. Biol.* **10**, 105–113 (2016).
13. K. L. B. Borden, L. Volpon, The diversity, plasticity, and adaptability of cap-dependent translation initiation and the associated machinery. *RNA Biol.* **17**, 1239–1251 (2020).
14. A. C. Gingras, S. G. Kennedy, M. A. O'Leary, N. Sonenberg, N. Hay, 4E-BP1, a repressor of mRNA translation, is phosphorylated and inactivated by the Akt(PKB) signaling pathway. *Genes Dev.* **12**, 502–513 (1998).
15. I. Ryu, Y. K. Kim, Translation initiation mediated by nuclear cap-binding protein complex. *BMB Rep.* **50**, 186–193 (2017).
16. G. Y. Liu, D. M. Sabatini, mTOR at the nexus of nutrition, growth, ageing and disease. *Nat. Rev. Mol. Cell Biol.* **21**, 183–203 (2020).
17. H. Chi, Regulation and function of mTOR signalling in T cell fate decisions. *Nat. Rev. Immunol.* **12**, 325–338 (2012).

18. C. de la Parra *et al.*, A widespread alternate form of cap-dependent mRNA translation initiation. *Nat. Commun.* **9**, 3068 (2018).
19. K. M. Kim *et al.*, A new MIF4G domain-containing protein, CTIF, directs nuclear cap-binding protein CBP80/20-dependent translation. *Genes Dev.* **23**, 2033–2045 (2009).
20. A. S. Lee, P. J. Kranzusch, J. A. Doudna, J. H. D. Cate, eIF3d is an mRNA cap-binding protein that is required for specialized translation initiation. *Nature* **536**, 96–99 (2016).
21. G. Singh, S. E. Fritz, B. Seufzer, K. Boris-Lawrie, The mRNA encoding the JUND tumor suppressor detains nuclear RNA-binding proteins to assemble polysomes that are unaffected by mTOR. *J. Biol. Chem.* **295**, 7763–7773 (2020).
22. A. Gebhardt *et al.*, mRNA export through an additional cap-binding complex consisting of NCBP1 and NCBP3. *Nat. Commun.* **6**, 8192 (2015).
23. A. Gebhardt *et al.*, The alternative cap-binding complex is required for antiviral defense in vivo. *PLoS Pathog.* **15**, e1008155 (2019).
24. J. Leblanc, J. Weil, K. Beemon, Posttranscriptional regulation of retroviral gene expression: Primary RNA transcripts play three roles as pre-mRNA, mRNA, and genomic RNA. *Wiley Interdiscip. Rev. RNA* **4**, 567–580 (2013).
25. S. Iacampo, A. Cochrane, Human immunodeficiency virus type 1 Rev function requires continued synthesis of its target mRNA. *J. Virol.* **70**, 8332–8339 (1996).
26. D. Toro-Ascuy *et al.*, A Rev-CBP80-eIF4AI complex drives Gag synthesis from the HIV-1 unspliced mRNA. *Nucleic Acids Res.* **46**, 11539–11552 (2018).
27. J. D. Short, C. M. Pfarr, Translational regulation of the JunD messenger RNA. *J. Biol. Chem.* **277**, 32697–32705 (2002).
28. C. C. Thoreen *et al.*, An ATP-competitive mammalian target of rapamycin inhibitor reveals rapamycin-resistant functions of mTORC1. *J. Biol. Chem.* **284**, 8023–8032 (2009). Correction in: *J. Biol. Chem.* **295**, 2886 (2020).
29. Q. Liu *et al.*, Discovery of 1-(4-(4-propionylpiperazin-1-yl)-3-(trifluoromethyl)phenyl)-9-(quinolin-3-yl)benzo[h][1,6]naphthyridin-2(1H)-one as a highly potent, selective mammalian target of rapamycin (mTOR) inhibitor for the treatment of cancer. *J. Med. Chem.* **53**, 7146–7155 (2010).
30. A. Heredia *et al.*, Targeting of mTOR catalytic site inhibits multiple steps of the HIV-1 lifecycle and suppresses HIV-1 viremia in humanized mice. *Proc. Natl. Acad. Sci. U.S.A.* **112**, 9412–9417 (2015).
31. E. Besnard *et al.*, The mTOR complex controls HIV latency. *Cell Host Microbe* **20**, 785–797 (2016).
32. H. E. Taylor *et al.*, mTOR overcomes multiple metabolic restrictions to enable HIV-1 reverse transcription and intracellular transport. *Cell Rep.* **31**, 107810 (2020).
33. A. Monette *et al.*, Dual mechanisms of translation initiation of the full-length HIV-1 mRNA contribute to gag synthesis. *PLoS One* **8**, e68108 (2013).
34. B. K. Felber, M. Hadzopoulou-Cladaras, C. Cladaras, T. Copeland, G. N. Pavlakis, rev protein of human immunodeficiency virus type 1 affects the stability and transport of the viral mRNA. *Proc. Natl. Acad. Sci. U.S.A.* **86**, 1495–1499 (1989).
35. C. Bolinger *et al.*, RNA helicase A interacts with divergent lymphotropic retroviruses and promotes translation of human T-cell leukemia virus type 1. *Nucleic Acids Res.* **35**, 2629–2642 (2007).
36. B. B. Roy *et al.*, Association of RNA helicase a with human immunodeficiency virus type 1 particles. *J. Biol. Chem.* **281**, 12625–12635 (2006).
37. I. Boeras *et al.*, DHX9/RHA binding to the PBS-segment of the genomic RNA during HIV-1 assembly bolsters virion infectivity. *J. Mol. Biol.* **428**, 2418–2429 (2016).
38. S. Brady *et al.*, Virion-associated, host-derived DHX9/RNA helicase A enhances the processivity of HIV-1 reverse transcriptase on genomic RNA. *J. Biol. Chem.* **294**, 11473–11485 (2019).
39. C. B. Buck *et al.*, The human immunodeficiency virus type 1 gag gene encodes an internal ribosome entry site. *J. Virol.* **75**, 181–191 (2001).
40. R. Amorim, S. M. Costa, N. P. Cavaleiro, E. E. da Silva, L. J. da Costa, HIV-1 transcripts use IRES-initiation under conditions where Cap-dependent translation is restricted by poliovirus 2A protease. *PLoS One* **9**, e88619 (2014).
41. A. Brasey *et al.*, The leader of human immunodeficiency virus type 1 genomic RNA harbors an internal ribosome entry segment that is active during the G2/M phase of the cell cycle. *J. Virol.* **77**, 3939–3949 (2003).
42. T. Ohlmann, C. Mengardi, M. López-Lastra, Translation initiation of the HIV-1 mRNA. *Translation (Austin)* **2**, e960242 (2014). Correction in: *Translation (Austin)* **3**, e1011549 (2015).
43. L. Hidalgo, C. M. Swanson, Regulation of human immunodeficiency virus type 1 (HIV-1) mRNA translation. *Biochem. Soc. Trans.* **45**, 353–364 (2017).
44. T. R. Hartman *et al.*, RNA helicase A is necessary for translation of selected messenger RNAs. *Nat. Struct. Mol. Biol.* **13**, 509–516 (2006).
45. C. Bolinger, A. Sharma, D. Singh, L. Yu, K. Boris-Lawrie, RNA helicase A modulates translation of HIV-1 and infectivity of progeny virions. *Nucleic Acids Res.* **38**, 1686–1696 (2010).
46. Z. Song *et al.*, The three-way junction structure of the HIV-1 PBS-segment binds host enzyme important for viral infectivity. *Nucleic Acids Res.* **49**, 5925–5942 (2021).
47. J. S. Gibbs *et al.*, Progression to AIDS in the absence of a gene for vpr or vpx. *J. Virol.* **69**, 2378–2383 (1995).
48. C. Bolinger, K. Boris-Lawrie, Mechanisms employed by retroviruses to exploit host factors for translational control of a complicated proteome. *Retrovirology* **6**, 8 (2009).
49. I. Ventoso, R. Blanco, C. Perales, L. Carrasco, HIV-1 protease cleaves eukaryotic initiation factor 4G and inhibits cap-dependent translation. *Proc. Natl. Acad. Sci. U.S.A.* **98**, 12966–12971 (2001).
50. E. Álvarez, A. Castelló, L. Menéndez-Arias, L. Carrasco, HIV protease cleaves poly(A)-binding protein. *Biochem. J.* **396**, 219–226 (2006).
51. A. Castelló *et al.*, HIV- 1 protease inhibits Cap- and poly(A)-dependent translation upon eIF4GI and PABP cleavage. *PLoS One* **4**, e7997 (2009).
52. T. Weichhart *et al.*, The TSC-mTOR signaling pathway regulates the innate inflammatory response. *Immunity* **29**, 565–577 (2008).
53. A. S. Y. Lee, P. J. Kranzusch, J. H. D. Cate, eIF3 targets cell-proliferation messenger RNAs for translational activation or repression. *Nature* **522**, 111–114 (2015).
54. M. J. Walker, M. D. Shortridge, D. D. Albin, L. Y. Cominsky, G. Varani, Structure of the RNA specialized translation initiation element that recruits eIF3 to the 5′-UTR of c-Jun. *J. Mol. Biol.* **432**, 1841–1855 (2020).
55. E. Amiel *et al.*, Inhibition of mechanistic target of rapamycin promotes dendritic cell activation and enhances therapeutic autologous vaccination in mice. *J. Immunol.* **189**, 2151–2158 (2012).
56. J. D. Brown, *et al.*, Structural basis for transcriptional start site control of HIV-1 RNA fate. *Science* **368**, 413–417 (2020).
57. I. Boeras *et al.*, The basal translation rate of authentic HIV-1 RNA is regulated by 5'UTR nt-pairings at junction of R and U5. *Sci. Rep.* **7**, 6902 (2017).
58. M. Butsch, S. Hull, Y. Wang, T. M. Roberts, K. Boris-Lawrie, The 5′ RNA terminus of spleen necrosis virus contains a novel posttranscriptional control element that facilitates human immunodeficiency virus Rev/RRE-independent Gag production. *J. Virol.* **73**, 4847–4855 (1999).
59. S. Hull, K. Boris-Lawrie, RU5 of Mason-Pfizer monkey virus 5′ long terminal repeat enhances cytoplasmic expression of human immunodeficiency virus type 1 gag-pol and nonviral reporter RNA. *J. Virol.* **76**, 10211–10218 (2002).
60. S. Kharytonchyk *et al.*, Transcriptional start site heterogeneity modulates the structure and function of the HIV-1 genome. *Proc. Natl. Acad. Sci. U.S.A.* **113**, 13378–13383 (2016).
61. P. S. Osmer, G. Singh, K. Boris-Lawrie, A new approach to 3D modeling of inhomogeneous populations of viral regulatory RNA. *Viruses* **12**, 1108 (2020).
62. G. Singh *et al.*, Identification of conserved, primary sequence motifs that direct retrovirus RNA fate. *Nucleic Acids Res.* **46**, 7366–7378 (2018).